SUPPORT SYSTEM FOR THE 1 m ESO ACTIVE OPTICS EXPERIMENT

O. Citterio, G. Conti, E. Mattaini
CNR-Istituto Fisica Cosmica
Milan, Italy

F. Franza,
ESO, Garching FRG

Introduction

The aim of this paper is to describe the support system which has been realized for the 1 m ESO active optics experiment. This experiment has been conceived in order to verify on a smaller scale the concept of the active optics, which is foreseen for the ESO NTT 3.5 m telescope. This concept has been widely discussed in references (1) (2) (3).

For the purpose of completeness we will briefly summarize here the basic concept of the experiment, while we will describe in detail the support system and the characterization of the force actuator.

Basic concept

The aim of the active optics control for the NTT telescope is to correct quasi-stable low spatial frequency aberrations of the optical system, physically related to the flexure of the mirror, and of the mechanical structure.

By implementing these features in the design of the telescope, it is expected to obtain the following results (2):

- automatic maintenance of the optics in quasi-real time
- possible relaxation of the manufacturing tolerances of the mirror and of the metallic structure
- lightening of the primary mirror and possible cheaper mirror materials.

The type of active control foreseen for the NTT telescope is based on the principle to use, for each low spatial frequency aberration to be corrected, a precalculated correction matrix and to determine, by linear superposition, the

Proceedings of the IAU Colloquium No. 79: "Very Large Telescopes, their Instrumentation and Programs", Garching, April 9–12, 1984.

https://doi.org/10.1017/S0252921100108255 Published online by Cambridge University Press

changes to be applied to the forces exerted by the actuators supporting the primary mirror (1) (2) (3). The design of the support system is consequently based on variable force actuators.

The scheme of the 1 m active optics experiment is shown in Fig. 1. It is foreseen that the primary mirror will work with the optical axis vertical. For the analysis of the wavefront, the Shack-Hartmann method (4) is used; the pupil is projected on a lens raster sampling the pupil with up to 850 points.

The image analyzer, which has as input sensor a CCD device, gives the coordinates of the points of the Hartmann image; after the reconstruction of the wavefront, this is analysed by means of a quasi-Zernike polynomial, as discussed in paper (2).

The precalculated correction matrix foreseen for each aberration which is intended to be corrected is multiplied by the aberration coefficients determined by the quasi-Zernike polynomial analysis. These quantities, which constitute the amount of force changes that must be applied to the actuators for each aberration, are linearly added (taking account of the relative azimuthal phase of the aberrations) and stored in the microprocessor memory. Through a multiplexer, these data are sequentially sent to the actuators that are required to update the force exerted.

The support assembly

Because the mirror is assumed to operate with the optical axis vertically oriented, no radial support system is required. The position of the axial actuators has been obtained by scaling down the configuration designed for the 3.5 NTT mirror (3) and has been also studied by finite elements calculation (5).

As shown by Fig. 2 there are 75 actuators, plus 3 fixed points, distributed on four concentric rings. The three fixed points, which incorporate a force sensor like the other 75 actuators, can be vertically adjusted.

The mirror has a diameter of 1050 mm and a thickness of about 18 mm; this thickness has been scaled down to have the same gravity flexure as the 3.5 m NTT primary mirror.

https://doi.org/10.1017/S0252921100108255 Published online by Cambridge University Press

All the actuators are fixed on a base plate; its rigidity need not be very high because of the astatic principle on which the actuators are based. The mirror is kept centered by means of three centering devices. Figs. 3 and 4 show respectively the assembled support system without and with the mirror which is still in the grinding phase.

The actuators

The characteristics requested for the design of the actuators were the following:

- nominal force: 500 gr
- change in the nominal force of ± 10% by means of a servocommand
- force repeatability better than 0.1% full scale (F.S.)
- must be based on the astatic principle and incorporate a force sensor
- must have a compact structure and low cost

Fig. 5 shows the mechanical scheme of the actuators that have been realized and Fig. 6 a photo of the system. They are based on the principle of a single lever. Provided that the contact point with the mirror, the axis of the shaft of the lever and the center of gravity of the counterweight are on the same line, this configuration presents an astatic behaviour.

The force which is transmitted to the mirror by means of the rotating ball is composed by a constant component given by the fixed counterweight plus a variable component given by the mobile weight, the translation of which is obtained through a small geared DC motor connected by a coupling joint to the precision micrometric screw. The exerted force is measured by the load cell on top of which the rotating ball is mounted.

As pivot devices for the lever, two small ball bearings (RIV-SKF 623) and flexural pivots (Bendix 5012-800) have been examined. Because, as will be seen later, the ball bearings have shown a friction characteristic which is compatible with the requested repeatibility figure, they have been selected on account of their better astatic behaviour (the flexural pivot gives a torque couple which is proportional to the angular rotation of the lever).

https://doi.org/10.1017/S0252921100108255 Published online by Cambridge University Press

The load cell is strongly sensitive to possible lateral components of the force to be measured. For this reason the force exerted by the actuator is applied to the mirror by means of a "rotating ball". This device is composed of a ball which rests on a bed of small balls. These smaller balls are housed in a spherical case. Although this configuration, as it will be shown later, behaves, from the point of view of the hysteresis, worse than a ball bearing, it has been selected because it takes care of the possible lateral friction forces independently of the direction.

The load cells that have been used present an intrinsic hysteresis which is better than 0.03% F.S.

Characterization of the actuators

Fig. 7 shows the results of the test performed to study the hysteresis behaviour of the actuator with different combinations of pivots and contact point devices.

In this test the mobile weight is translated between the two extreme positions in 13 incremental steps. The position of the mobile weight is measured by counting the number of revolutions of the motor shaft by means of a fiber optics probe. The total change in force is ± 45 gr.

Three complete forward and backward cycles are made; for the position where the force is measured, the average values are reported together with the standard error bars. For the average values of each position, the related nominal increment of force has been subtracted, consequently on the diagrams the differences are indicated between the exerted forces in the forward and backward conditions. For a perfect system the diagram should be a straight line.

Fig. 7a and 7b compare the results of two actuators using ball bearings and a rotating ball for transmitting the force to the mirror. The worse hysteresis effect presented by the configuration with the rotating ball is clearly shown.

Examination of this behaviour has shown that the change of the exerted force produces on the load cell a slight flexure modification to which corresponds a small rotation of the lever. This rotation is accompanied, during the inversion of the movement, by a small lateral displacement of the ball in its housing

https://doi.org/10.1017/S0252921100108255 Published online by Cambridge University Press

which causes a small change in the arms of the lever. As has already been said, despite this worse behaviour, the rotating ball has been selected because it is free from the problem of lateral frictional forces.

Fig. 7a and 7c compare the results of two actuators using a ball bearing for transmitting the force to the mirror and a ball bearing or a flexural pivot as shaft for the lever. As expected, the flexural pivot shows the best hysteresis performances. Nevertheless the difference with respect to the ball bearing is not very high. Looking at the error bars on the diagram, it is possible to derive the force repeatibility characteristic of the different configurations. Fig. 7b and 7d show a similar comparison with the rotating ball.

Fig. 8 shows the results of the tests performed to study the astatic behaviour of the actuators. In this test, the plane of reaction (simulating the mirror) is vertically translated; the values of the exerted force are taken for several different positions of the reaction plane, which are measured by a dial gauge.

Fig. 8a and 8b compare the results of two actuators using a ball bearing and a rotating ball for transmitting the force to the reaction plane. On the two diagrams the straight line represents the best fit of the measured values. The slope of this line is taken as the coefficient of non-astaticity; the non-zero value of this slope means that the point of contact with the reaction plane, the axis of the shaft of the lever and the center of gravity of the counterweight are not on the same line; this is due to the fact that the mobile weight changes the position of the center of gravity of the total counterweight.

The noisy distribution of the measured values around the best fit line is due to microsettlement of the ball bearing or of the rotating ball, transmitting the force to the reaction plane. As expected, the rotating ball gives the highest noise.

To verify that there is not a significant contribution to the noise due to the possible friction component of the ball bearing mounted on the axis of the lever, the actuator has been tested with the configuration of Fig. 9a and 9b where the actuator is coupled to the reaction plane through a piece of wire. Diagrams 9a and 9b clearly show the noise-free relation between the translation of the reaction plane and the measured values of the force. Fig. 9b shows also that with a flexural pivot mounted on the axis of the lever, the coefficient of non-astaticity becomes worse by about a factor of two.

https://doi.org/10.1017/S0252921100108255 Published online by Cambridge University Press

Conclusions

A summary of the characteristics of the actuators with different configurations is given in Table 1. The configuration with ball bearing for the shaft of the lever and rotating ball for transmitting the force has been selected because it reaches our design goal for maximum repeatability error of better than 0.1% and has the advantage of avoiding the effect of the lateral forces on the load cell.

It is important to point out that the effect of this possible lateral force together with the intrinsic accuracy of the load cell, are the most important parameters which limit the accuracy in the measurement of the exerted force; in fact while the non-astaticity coefficient and the hysteresis are important parameters to be considered in the case of actuators operating in an open loop, in this experiment they are automatically corrected by the fact that the exerted force is measured in quasi-real time by the load cell which is included in a closed regulation loop.

Acknowledgements

The development of this work has benefited from helpful discussions with many ESO colleagues, particularly K. Mischung, L. Noethe, M. Tarenghi, R. Wilson and M. Ziebell, to whom we express our sincere thanks.

https://doi.org/10.1017/S0252921100108255 Published online by Cambridge University Press

References

(1) R.N. Wilson, "Image quality considerations in ESO telescope projects", Optical Acta, 1982, Vol. 29, No. 7, 985-992.

(2) R.N. Wilson, "Image quality and high resolution in future telescopes", Proceedings of the ESO conference on "Scientific importance of high angular resolution at I.R. and optical wavelengths", Munich, 1981, 67-83.

(3) F. Franza, R.N. Wilson, "Status of the European Southern Observatory New Technology Telescope Project", SPIE Proceedings, Vol. 332, "Advanced Technology Optical Telescopes", Tucson, 1982, 90-101.

(4) R.N. Wilson, F. Franza, L. Noethe, M. Tarenghi, "The ESO off-line telescope testing technique illustrated with results for the MPIA 2,2 m Telescope II", Proceedings of this Conference.

(5) G. Ballio, O. Citterio, R. Contro and C. Poggi, "A finite element approach to the design of the support system for the ESO 1 m active optics experiment", Proceedings of this Conference.

https://doi.org/10.1017/S0252921100108255 Published online by Cambridge University Press

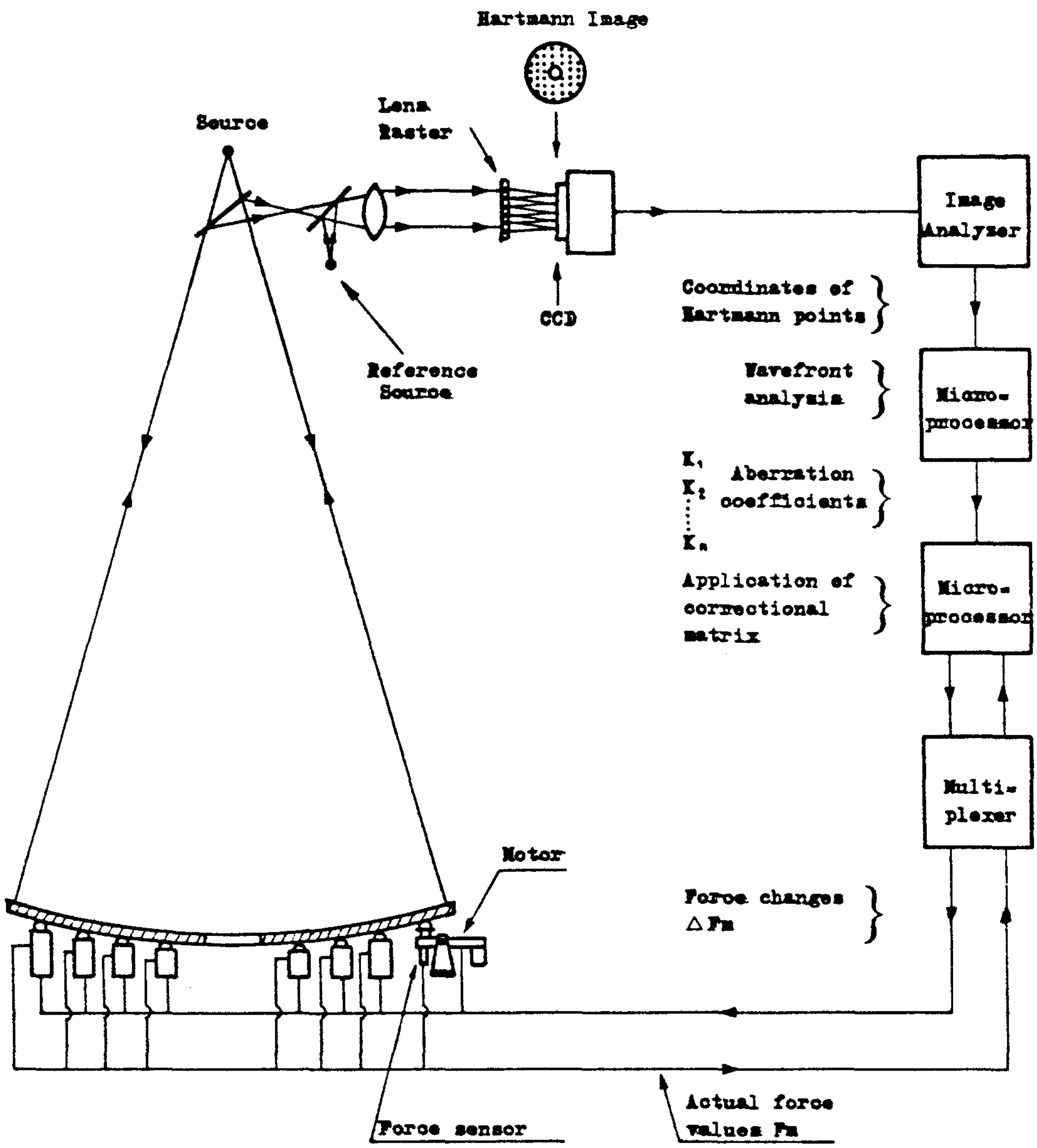

Fig. 1 Scheme of the 1 m ESO active optics experiment.

https://doi.org/10.1017/S0252921100108255 Published online by Cambridge University Press

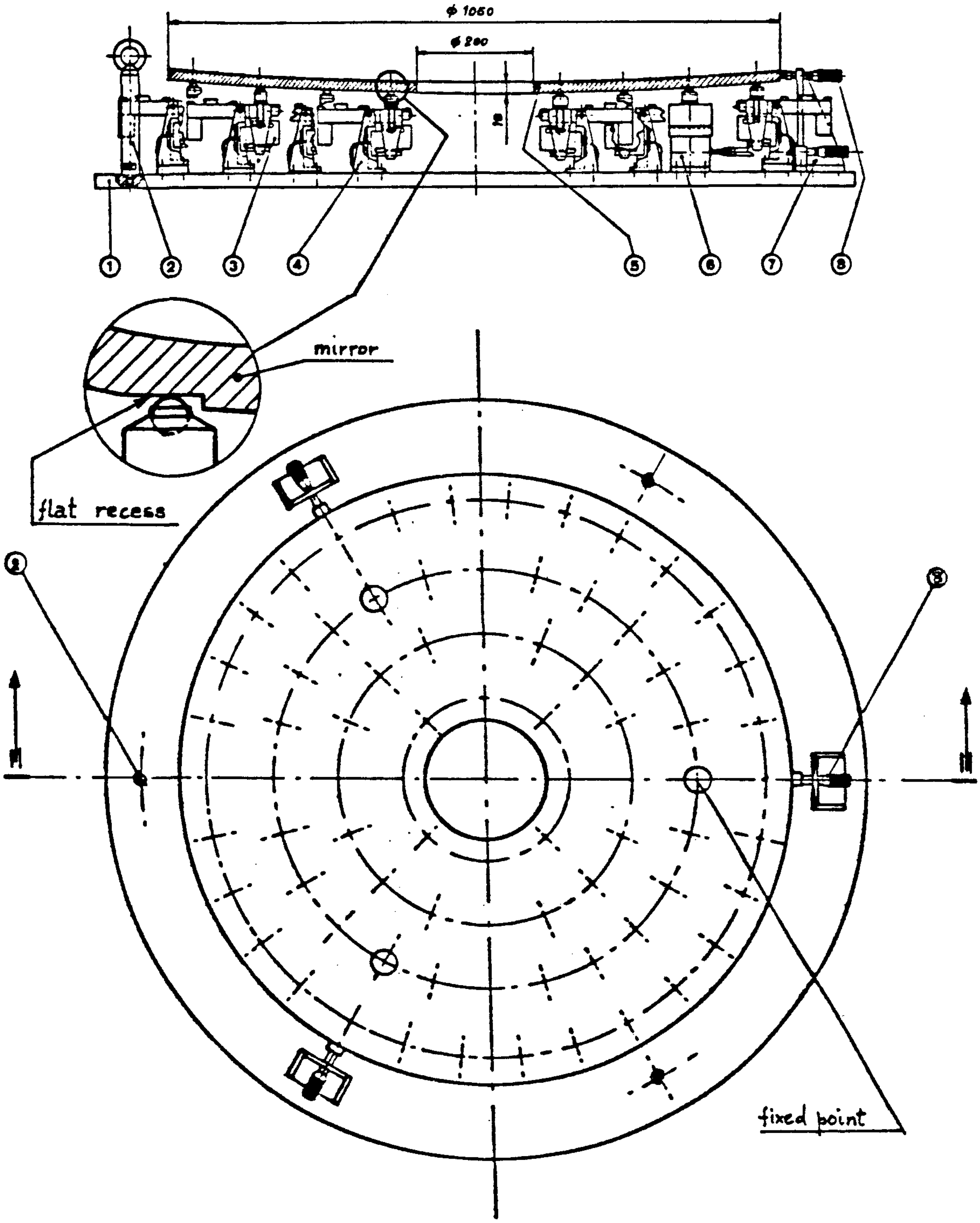

Fig. 2
I) Base plate 2) Lifting hook 3) Load cell 4) Actuator
5) Mirror 6) Regulation system for fixed point 7) Support
for radial centering 8) Radial centering device

https://doi.org/10.1017/S0252921100108255 Published online by Cambridge University Press

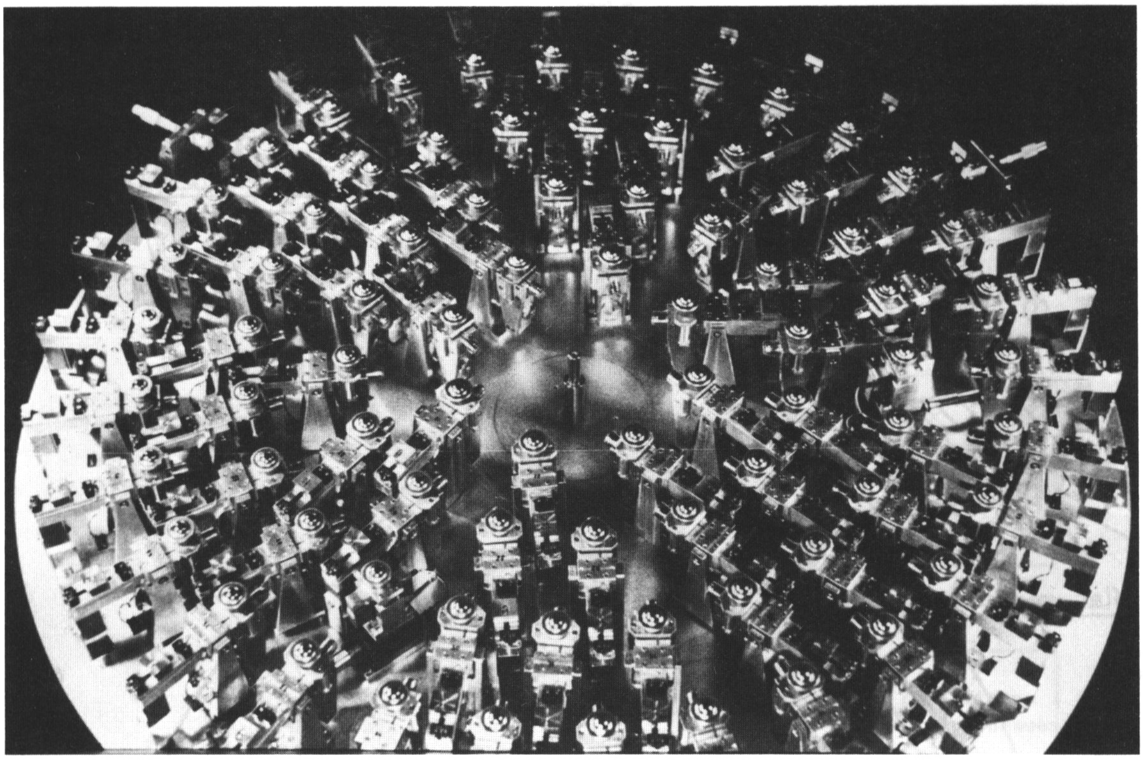

Fig. 3 Photograph of the support system

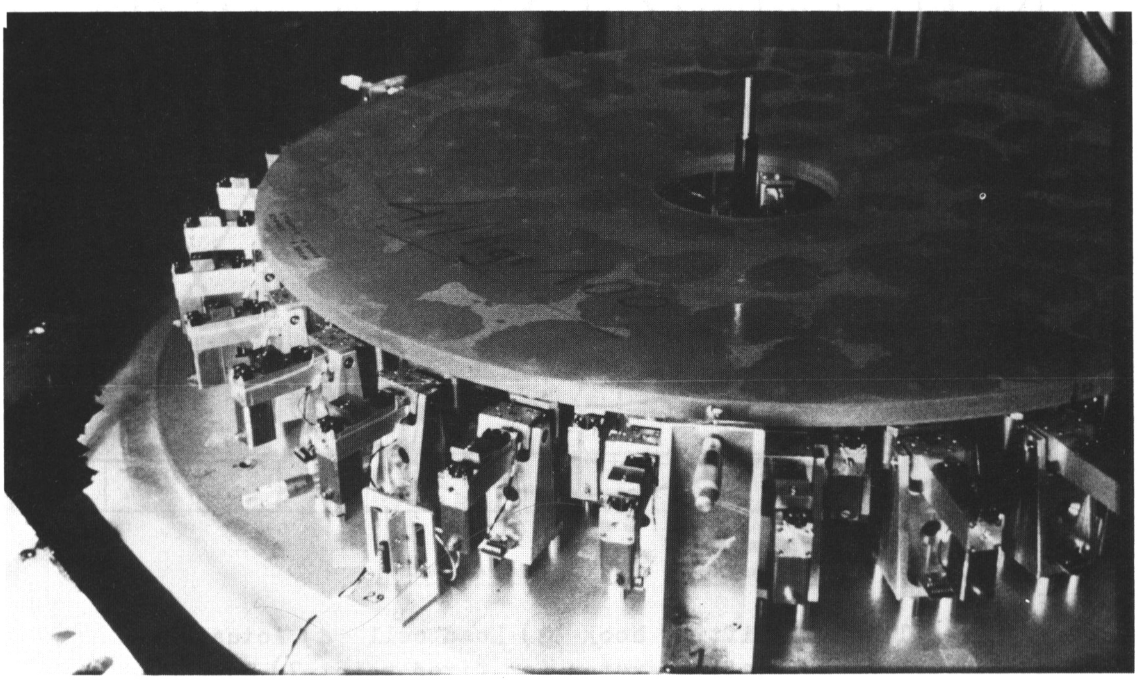

Fig. 4 Photograph of the support system with the mirror. The mirror is not yet polished.

https://doi.org/10.1017/S0252921100108255 Published online by Cambridge University Press

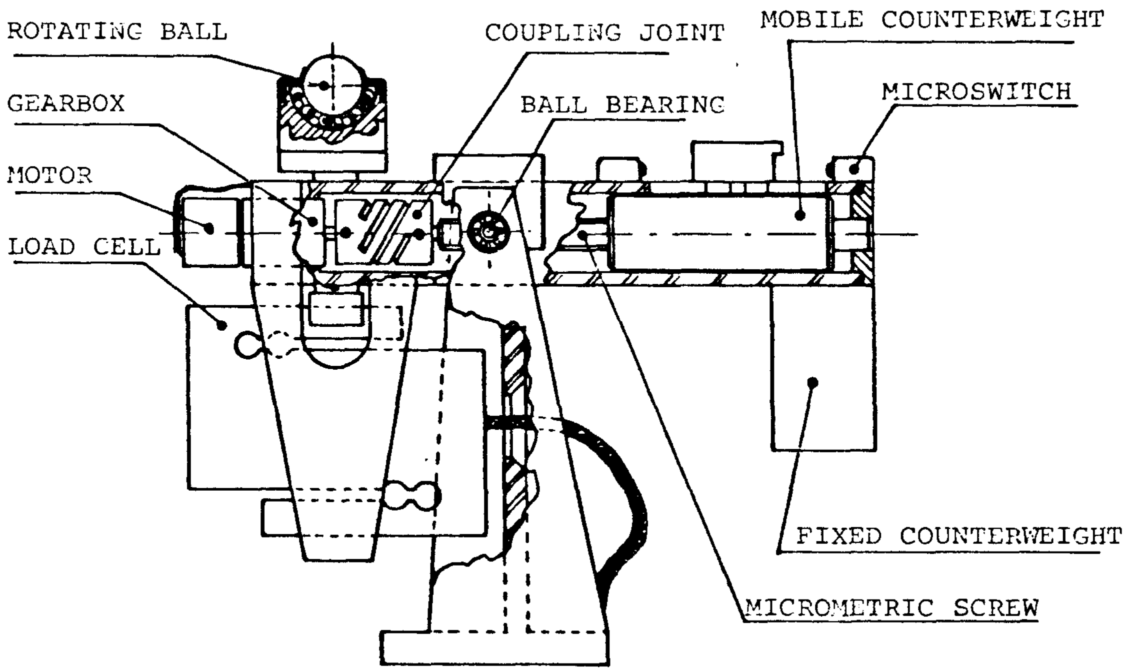

Fig. 5 Mechanical scheme of the actuator

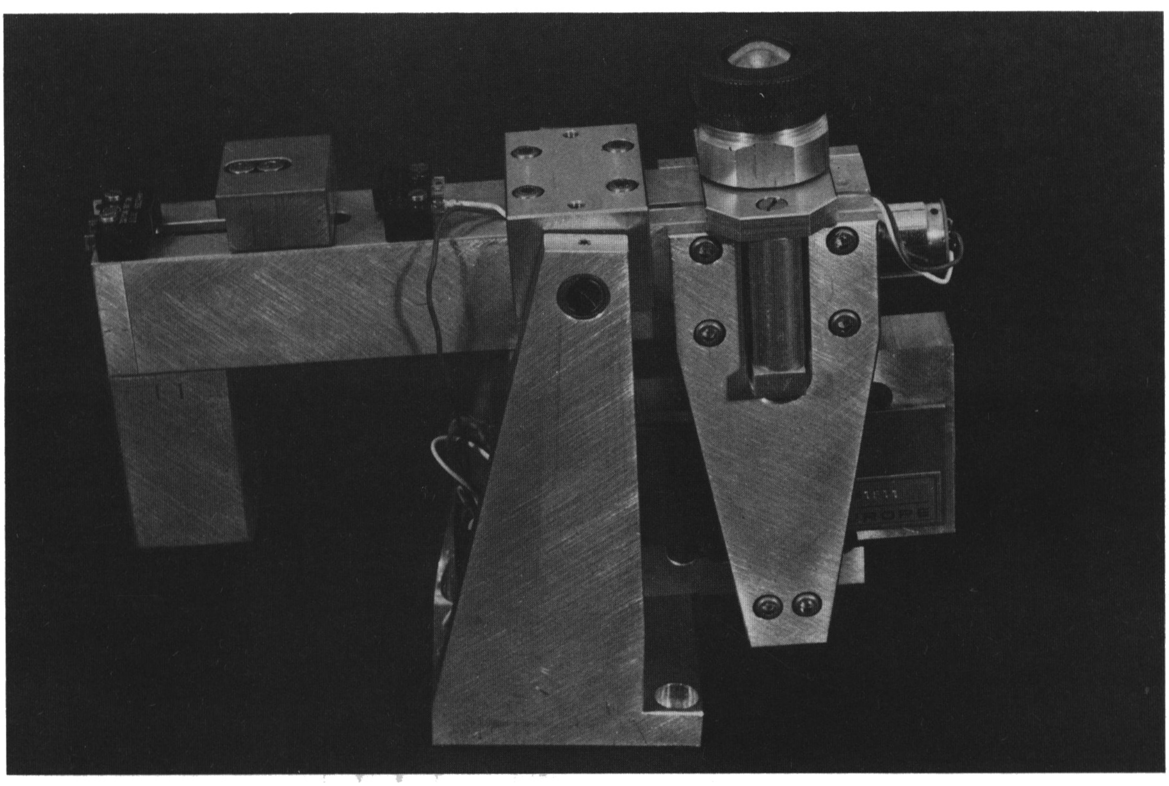

Fig. 6 Photograph of the actuator

https://doi.org/10.1017/S0252921100108255 Published online by Cambridge University Press

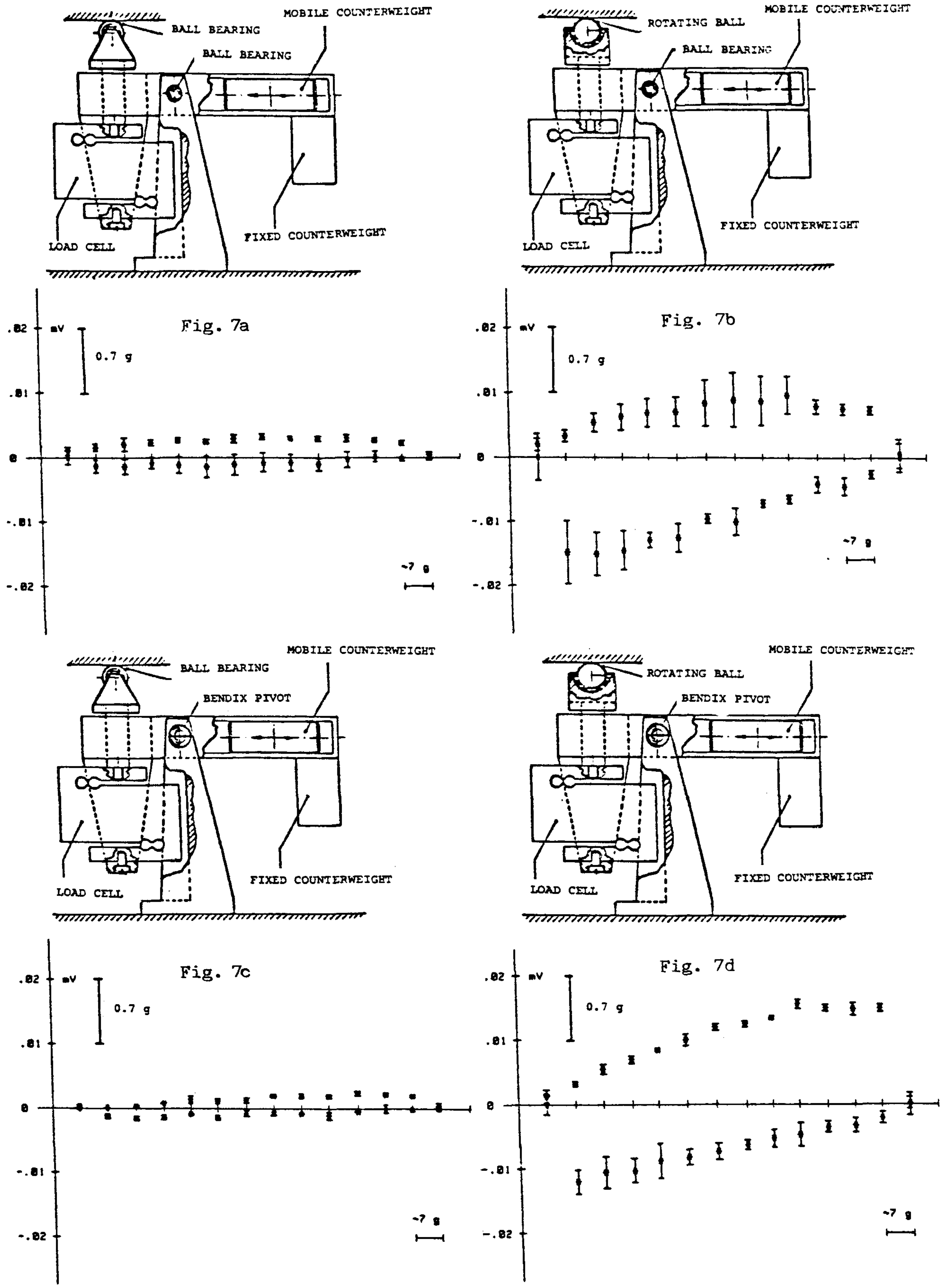

Fig. 7 Hysteresis test on actuators with different configurations.

https://doi.org/10.1017/S0252921100108255 Published online by Cambridge University Press

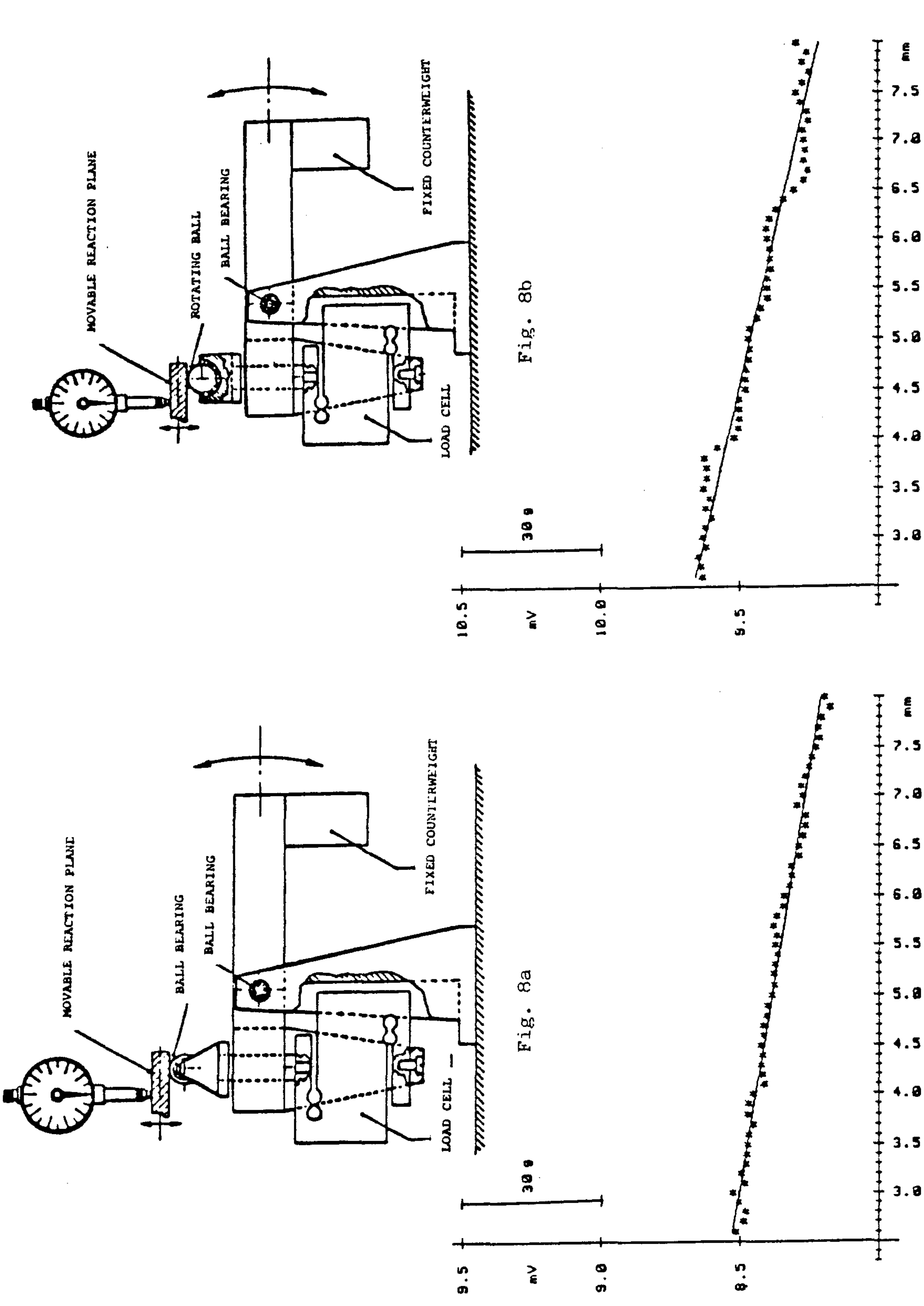

Fig.8 Astaticity test on two actuators with different devices for transmitting the force to the reaction plane

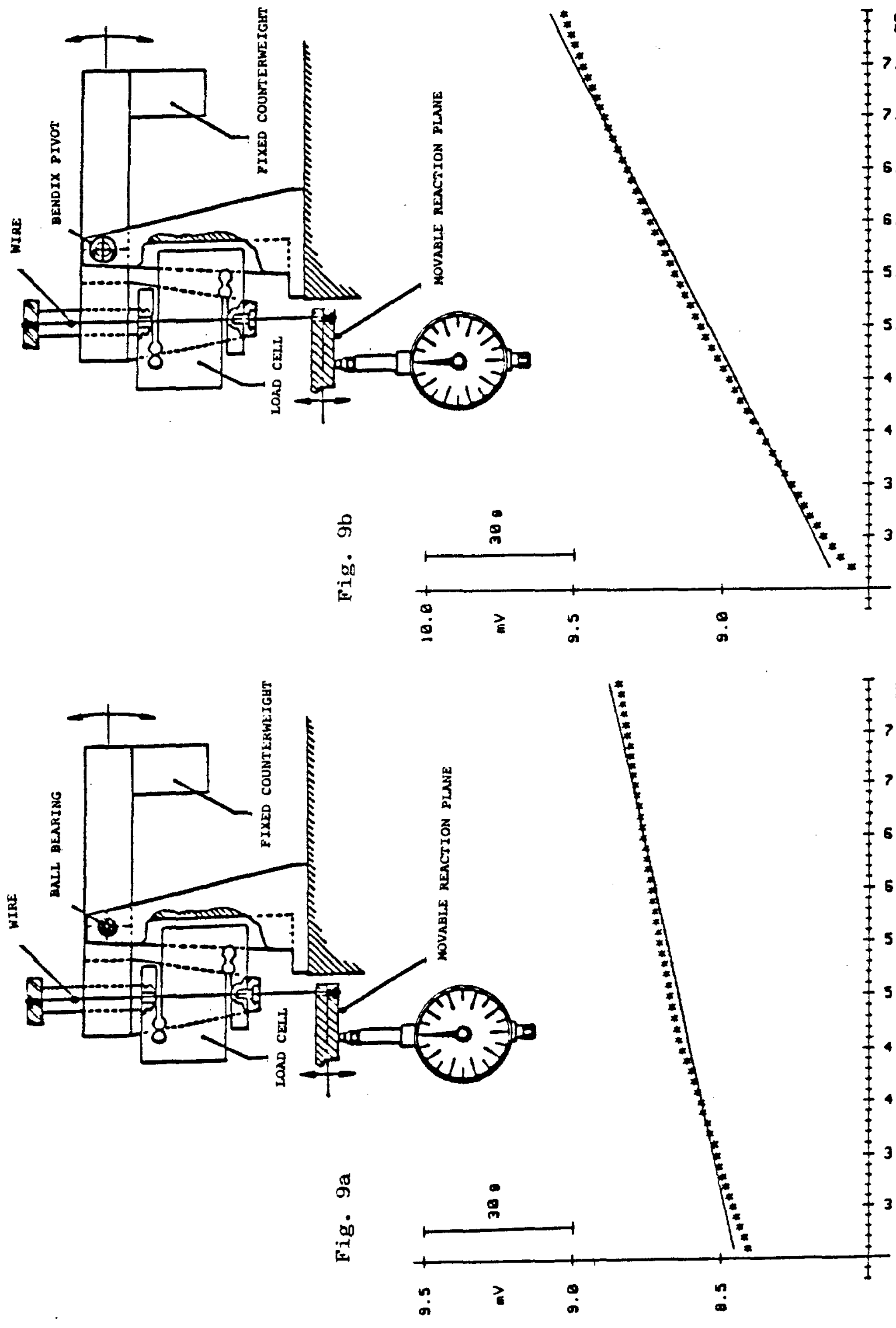

Fig.9 Astaticity test on two actuators with different pivot devices. The force is transmitted to the reaction plane by a wire

https://doi.org/10.1017/S0252921100108255 Published online by Cambridge University Press

PIVOT DEVICE	MIRROR CONTACT DEVICE	MEAN HYSTERESIS		NON-ASTATICITY COEFFICIENT	MAXIMUM ERROR OF REPEATABILITY	
		grams	% error	grams/mm	grams	% error
FLEXURAL PIVOT	BALL BEARING	0.15	0.030	7.06	± 0.04	±0.008
	SPHERE	1.15	0.230	9.76	± 0.16	±0.032
BALL BEARING	BALL BEARING	0.23	0.046	3.54	± 0.10	±0.020
	SPHERE	1.09	0.220	4.95	± 0.30	±0.060

Table 1. Summary of the characteristics of actuators with different configurations.

https://doi.org/10.1017/S0252921100108255 Published online by Cambridge University Press

DISCUSSION

J. Nelson: (to O. Citterio concerning thickness of 1m NTT test mirror described by Citterio)

R. Wilson: The NTT 1m test mirror described by Oberto Citterio is only about 18mm thick because it has been scaled down from the full-sized 3.5m blank not linearly, but following the gravity flexure law proportional to D^4/d^2. Its support system is then identical in form to that of the full-sized mirror with loads scaled down according to the relative weights.

https://doi.org/10.1017/S0252921100108255 Published online by Cambridge University Press